Advanced Blast Chamber for Reproducible Blast Exposures at Full Scale: from subconcussive planar wave to high overpressure blasts with multiple reflections

Joseph Kerwin[1], Adam M. Willis, M.D., Ph.D, Maj, USAF[1,2] , and Ricardo Mejia-Alvarez, Ph.D[1],

Grant #: AFRL-FA8650-18-2-6880

1. Department of Mechanical Engineering, Michigan State University, East Lansing, MI 48824
2. Department of Neurology, San Antonio Military Medical Center, Fort Sam Houston, TX 78234

Purpose and Learning Objectives

Blast waves can induce intracranial localized stresses at tissue interfaces that could be responsible for damage in the neurons, glia, vasculature, and ventricular system [1,2]. To characterize the mechanics by which blast waves can cause severe brain injuries, we are conducting experimental measurements of the physics of intracranial interactions between skull contents and blast waves, using both human head surrogates, and in-vivo animal models.

Learning Objectives

1. Establishing links between wearable blast sensor data and traumatic brain injury pathology.
2. Assessing exposure severity on biofidelic phantoms of human anatomy to develop safe exposure standards.
3. Understanding the mechanics of blast induced traumatic brain injury with biofidelic phantoms and in-vivo animal models.

The ABC (Advanced Blast Chamber)

Figure 1. The ABC is a self-standing instrument composed by a blast chamber and a dissipation chamber. The blast chamber is sheltered by the structure on the right-hand-side, and the dissipation chamber is inside the sand berm on the left-hand-side.

Figure 2. The Blast Chamber is composed by a Driver Section (1.5m deep steel cavity encased in reinforced concrete) and a steel-made Test Section with cross-section 2m x 2m and length 5.5m. Total length: 7m. The chamber protrudes through the dividing wall into the Dissipation Chamber.

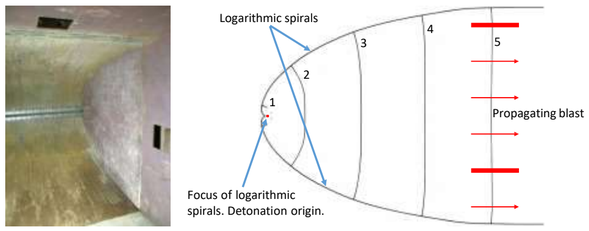

Figure 3. The Driver Section (left) is a concave acoustic mirror with two opposing logarithmic spirals as its generatrix (right). This geometry is such that a cylindrical blast originating at the common focus of the spirals will unfold into an almost flat blast (right, 5 stages of development) [3].

Figure 4. The end edges of the test section are serrated to start fragmenting the blast and to reduce noise (left) [4]. The blast is discharged into the dissipation chamber (right). The interior of this chamber is covered by 30 cm of rubber mulch to absorb and dissipate the energy of the blast.

Instrumentation and Analysis Techniques

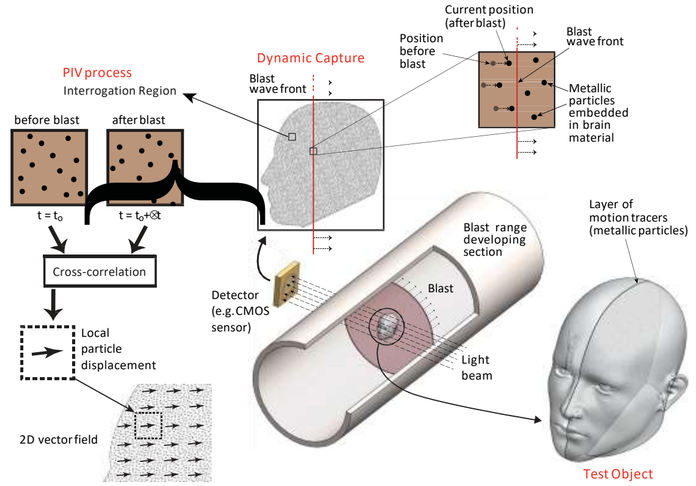

Figure 5. Dynamic measurements with ultra-high-speed imaging while the blast wave is crossing the test object (blast range on the center of the figure). The test object is a phantom of the human head with a layer of particles embedded in an inner plane (bottom-right). The embedded particles trace strain as the detonation wave propagates (center-top and zoomed-in view of the edge of the detonation wave, top-right). Particle Image Velocimetry (PIV) is used to generate 2D vector fields representing strain and strain-rate (schematic of PIV process on the left).

Scan Me
for more information

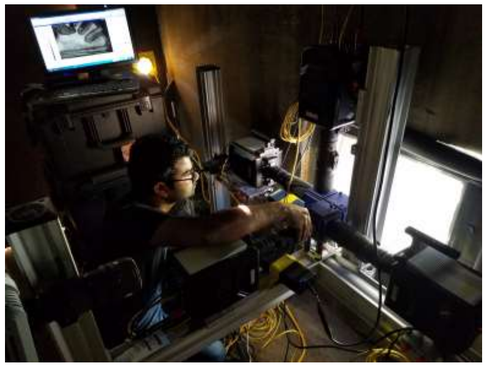

Figure 6. We use 4 ultrahigh-speed cameras Phantom V2512 with CMOS sensors of 1Mpixel, on-board memory of 144GB, maximum frame rate at maximum resolution of 25,700 fps, and more than 1,000,000 fps at reduced resolution. As shown, the cameras can be optically coupled and triggered in sequence to quadruple the available frame rate.

Figure 7. The current test object (1st generation) is a simplified dual-material phantom based on the dominant geometrical features of an axial cut of a real patient. The materials are two different grades of polyacrylamide, tailored to approximate the mechanical properties of white and gray matter.

Ongoing Experiments

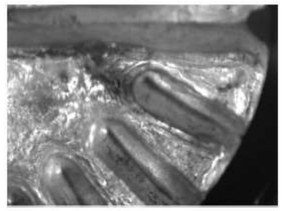

Figure 8. Zoomed-in view of the right hemisphere of the frontal region of the 1st generation test object. This location was also the *coup* under blast-loading.

Measurements using the first generation Test Object have so far confirmed that shear and normal strains tend to concentrate in the material interfaces between white and gray matter, consistent with pathology observed in cadaver studies [5].

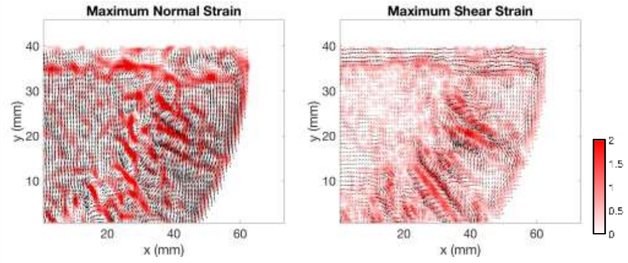

Figure 9. Calculations of maximum normal and shear strains using PIV. The vectors point in the local direction of strain and the contour maps give the magnitude. These results were obtained with a frontal blast-loading with an overpressure of 519kPa (75.2psi).

Future Experiments

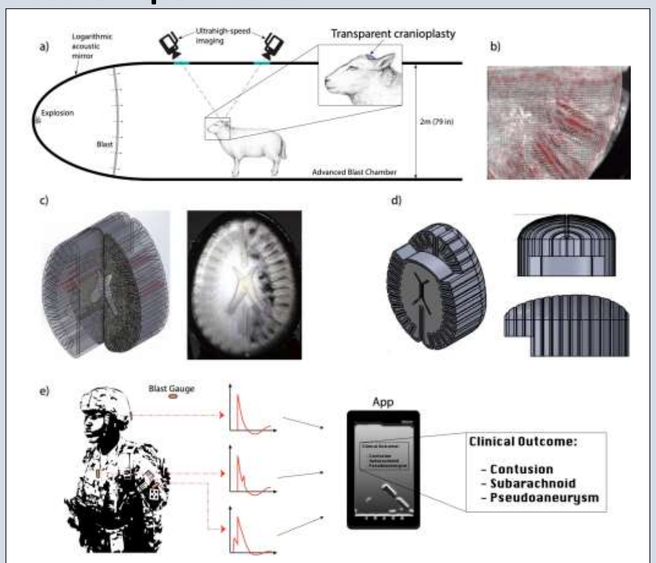

Figure 10. (a) and (b): establishing injury thresholds by measuring in vivo tissue deformation during blast injury and linking that to living bTBI ovine pathology; (c) and (d) validate phantom tissue models with in vivo experimental data to build a validated human head phantom for blast testing; (e) Isolate blast sensor data that correlates with a level of head phantom tissue deformation expected to cause injury based upon the in vivo data.

References

1. Ling, GSF and Ecklund, JM, Traumatic brain injury in modern war. Curr. Opin. Anaesthesiol., 24: 124-130, 2011.
2. Abdul-Muneer, P et al. Induction of oxidative and nitrosative damage leads to cerebrovascular inflammation in an animal model of mild traumatic brain injury induced by primary blast. Free Radic. Biol. Med., 60: 282-291, 2013.
3. Milton, BE. The focusing of shock waves in two dimensional and axi-symmetric ducts. In: Proc. Int. Workshop Shock Wave Focusing, Shock Wave Research Center, Inst. Fluid Sci., Tohoku University 1989 Mar.
4. Howe, M. S. Noise Produced by a Sawtooth Trailing Edge. The Journal of the Acoustical Society of America 90 (1): 482–87, 1991.
5. Willis, A. Visualizing and Quantifying the Kinematics of Blast Traumatic Brain Injury Pathology in a Preclinical Model. 2018 MHSRS.